

Evaluation of structural adhesive joints fracture toughness without crack measurement

Jonnas Santos Alves ¹, Paulo Pedro Kenedi ¹, Silvio de Barros ¹

¹Programa de Pós-Graduação em Engenharia Mecânica e Tecnologia de Materiais (PPEMM) CEFET/RJ, Av. Maracanã, 229, CEP 20271-110, Rio de Janeiro, RJ, Brazil
e-mail:tenjonas@gmail.com, paulo.kenedi@cefet-rj.br, silvio.debarros@gmail.com

ABSTRACT

The adhesive fracture resistance of structural adhesive joints in mode II, \mathcal{G}_{IIC} , is accessed through the application of two models that prescind of the measurement of the crack length during the subjection of ENF specimens to three-point bending monotonic tests. The load vs transversal displacement results are used in two different approaches: a damage model and a cohesive zone model. The first one was used in test where the crack propagation was unstable and the second one was used for stable crack propagations. These initial results show the viability of the models and show that both: initial crack length and transversal load rate; have great influence in \mathcal{G}_{IIC} evaluation.

Keywords: structural adhesive joints, ENF specimens, fracture mechanics.

1. INTRODUCTION

Structural adhesive joints are characterized by their simplicity and efficiency of use. The actual development of high mechanical resistance adhesives finds a significant place in industrial applications. In fact, the adhesive bonding can substitute traditional joints as rivets and screws, with the clear advantage of diminishing the stress concentration effects. One typical example of the use of structural adhesives can be found in repair of pipelines with loss of thickness caused by corrosion.

The objective of this work is evaluating the critical energy relief rate \mathcal{G}_{IIC} of the structural adhesives in mode II. To accomplish this goal, end notched flexure (ENF) specimens are used in the experimental part (where the adhesive is submitted to pure shear loading) and two different models: a proposed damage model and existent cohesive zone model.

Both theoretical approaches are based in Griffith model, which establish the rate of relief of elastic potential energy stored in the system \mathcal{G} , according to equation (1), as in [1]. The negative signal of this equation stands for the energy stored in the cracked part decreases as the crack increases its length.

$$\mathcal{G} = -\frac{\partial E_P}{\partial A} \quad (1)$$

Where E_P is the potential energy of the system. So, the energy relief rate is a property of the cracked structure and is defined by:

$$\mathcal{G} = \frac{P^2}{2B} \frac{dC}{da} \quad (2)$$

Where B is the width, P is the loading, $C = \delta / P$ is the compliance and a is the crack length.

There are many models that use equation (2) to access the fracture toughness of an adhesive joint. Unfortunately, most of these models needs the crack length measurement during the test. This fact is quite restrictive; once it is remarkably difficult to access the crack length during its stable growth.

In this work the equation (2) will be used, with solid mechanics beam theory, to assess the fracture toughness of structural adhesive joints in mode II, \mathcal{G}_{IIC} . So, to bypass the limitation of the other models that

needs the crack length measurement during the test, in this work it is proposed the use two different approaches that don't need the measurement of crack length during tests: a proposed analytical model based on the originally proposed damage model by ALLIX *et al.* [2], and improved by BARROS and CHAMPANEY [3 - 5]; and an existent cohesive zone model proposed by MOURA *et al.* [6 - 9]. See, also, other interesting papers of fracture toughness of structural adhesive joints [10 - 13].

The main tests used for crack opening in bonded joints in I, II and mixed mode (I + II) are commonly referred as DCB, ENF and MMF tests, respectively.

The DCB or mode I test is the most used in bonded joints and currently this type of test is standardized by ASTM D3433-99 [14] for \mathcal{G}_{IC} measurement. In this test it is considered an initial crack a_0 , and the tensile load that is applied perpendicular to crack. The crosshead speed of the test is set between 0.5 and 3 mm/min, depending on the geometry and the characteristics of the adhesive joint. During the test, the load P and displacement δ are recorded for the corresponding crack size values a in order to calculate the critical energy relief rate \mathcal{G}_{IC} . Fig. 1.a, schematically, shows a DCB test.

The MMF mode test is similar to the ENF test, however one of the ends of the specimen in the MMF test is supported only by the top bar, as shown in Fig. 1.c, subjecting the specimen to a tensile load (mode I) and a shear load (mode II) simultaneously.

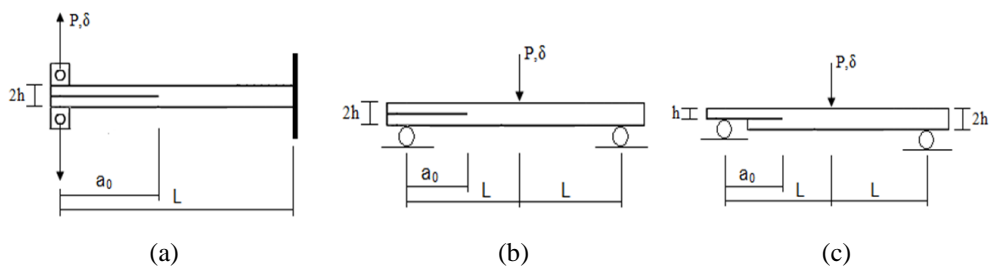


Figure 1: Schematic representation of specimens of the following tests: (a) DCB, (b) ENF and (c) MMF.

Due to its geometric simplicity, the ENF specimen is considered the most adequate to perform a mode II test, for the bonded joints fracture characterization, as shown in Fig. 1.b. However, this test presents certain complexity related to the unstable crack propagation, inherent difficulty in experimentally measuring the crack length and the existence of the Fracture Process Zone (ZPF). These difficulties can lead to errors in the experimentally measured value of \mathcal{G}_{IIC} . In order to overcome the difficulties reported in the ENF test, for instance, the influence of the energy released in the ZPF can be evaluated through the proposal of an equivalent crack concept, which depends only on the compliance C of the joint to obtain \mathcal{G}_{IIC} , CHAVES *et al.* [15].

1.1 Methods for determining \mathcal{G}_{IIC}

The fracture toughness of bonded joints, in mode II, \mathcal{G}_{IIC} , can be accessed by two classic methods: Compliance Calibration Method (CCM) or Direct Beam Theory (DBT), CHAVES *et al.* [15]. The CCM method is based on the Irwin-Kies equation, as shown in equation (2). In this method an adjustment (calibration) of compliance C is performed in function of flexural tests with different crack sizes. The adjustment of the curve $C = f(a)$ to the results is done using a cubic polynomial curve ($C = C_0 + ma^3$):

$$\mathcal{G}_{IIC} = \frac{3mP^2a^2}{2B} \quad (3)$$

Where the coefficient C_0 is the initial compliance and m is the slope of the curve C vs a^3 obtained by linear regression of the least square method.

An example of the Direct Beam Theory Method – DBT, uses beam theory and the \mathcal{G}_{IIC} and equation (2):

$$\mathcal{G}_{IIC} = \frac{9P\delta a^2}{2B(2L^3 + 3a^3)} \quad (4)$$

Where δ is the vertical displacement of the specimen.

There are also some alternative methods for calculating the fracture toughness as: the Corrected Beam Theory (CBT) and the Compliance Based Beam Method (CBBM). The first one is board in sequence and the second one, MOURA *et al.* [7], will be described, in details, in Material and Methods Section.

The Corrected Beam Theory Method - CBT, defines the \mathcal{G}_{IC} value as:

$$\mathcal{G}_{IC} = \frac{9P^2 a}{16B^2 E_f h^3} \frac{F}{N} f_v \quad (5)$$

Where h is half the height of the specimen, E_f is the flexural modulus, F and N are corrections factors for large displacements, for the moment arm and for compliance, respectively, and f_v includes the cross-shear effect.

The CCM, DBT and CBT approaches are methods that require the measurement of crack size, a , during the test, which is not a trivial task. As a result, important errors can occur during the characterization of bonded fracture under loading mode II. In fact, one of the most critical aspects of ENF testing is the great difficulty in measuring crack size during test.

2. MATERIALS AND METHODS

In this section two analytical models, that not need the crack length measurement during test, are presented: a proposed model (based in damage theory model) and an existent CBBM model (based in cohesive zone theory).

2.1 the proposed analytical model

The critical energy release rate \mathcal{G}_c can be used to model the behaviour of the bonded specimens during crack generation. To achieve this objective the application of the analytical model, which were originally proposed by ALLIX *et al.* [2] and improved by BARROS and CHAMPANEY [3 - 5], can be divided into two parts: a resistance part comprising the crack propagation curves, for various \mathcal{G}_c values, generated by the application of the classic beam theory together the Linear Elastic Fracture Mechanics (LEFM), as can be seen, for instance, in Fig. 5; and an experimental part represented by result of crack propagation of ENF specimens submitted to three point tests. Concepts of solids mechanics and LEFM are used to develop this analytical model by ALVES [12] are shown in this section. See, APPENDIX B to access the calculations used to determine the dimensions and the material of substrate selection to prevent yielding of substrate before adhesive rupture.

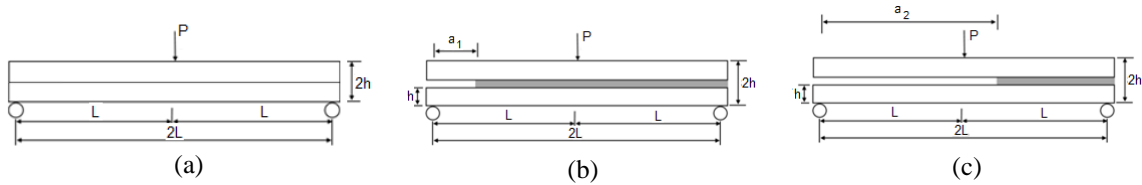


Figure 2: Schematic representation of the ENF test for: (a) $a_0 = 0$, (b) $0 \leq a_1 < L$ and (c) for $L \leq a_2 \leq 2L$.

Although the shearing stresses are the cause of failure of adhesive in specimen neutral region, at steel substrates the shearing stresses are considered not significative. So, only the bending strain energy is used to calculate the behaviour of two bonded bars submitted to a three-point bending test. Due to the existence of an initial crack, of length a_0 , in the adhesive interface, it is necessary separate the study in two parts: a region without adhesive, it is considered that there are two bars of h thickness each, and in the region with adhesive, there is only a single beam, with double thickness $2h$ (the adhesive thickness was not taken into account).

Thus, the elastic energy of the ENF specimen subjected to bending loading, for $0 \leq a_1 < L$, is:

$$E_d = \int_0^{a_1} \frac{M_1^2(x)}{2E(2I_1)} dx + \int_{a_1}^L \frac{M_1^2(x)}{2EI_2} dx + \int_L^{2L} \frac{M_2^2(x)}{2EI_2} dx = \frac{1}{2} P u_1 \quad (6)$$

Where, $M_1(x) = \frac{P}{2}x$, $0 \leq x < L$ and $M_2(x) = P\left(L - \frac{x}{2}\right)$, $L \leq x \leq 2L$; $I_1 = \frac{bh^3}{12} = I$ and $I_2 = \frac{B(2h)^3}{12} = 8I$. u_1 is the transversal displacement of ENF specimen at mid span. $M_1(x)$ and $M_2(x)$ are the bending moments. I_1 and I_2 are the moment of inertia. Applying Castigliano's theorem in equation (6):

$$u_1 = \frac{PL^3}{48EI} + \frac{Pa_1^3}{32EI} \quad (7)$$

Thus, the stiffness K and the compliance C of the specimen with crack are obtained:

$$K_1 = \frac{EI}{\frac{L^3}{48} + \frac{a_1^3}{32}} \quad C_1 = \frac{L^3}{48EI} + \frac{a_1^3}{32EI} \quad (8)$$

Using equation (8.b) in equation (2), \mathcal{G}_{IIC} can be estimated as:

$$\mathcal{G}_{IIC} = \frac{3P^2 a_1^2}{64BEI} \quad \text{or} \quad \mathcal{G}_{IIC} = \frac{9P^2 a_1^2}{16B^2 E h^3} \quad (9)$$

Rewriting equation (9.a) gives the value of the crack length a_1 in function of the energy relief rate:

$$a_1 = \frac{8}{P} \sqrt{\frac{BEI \mathcal{G}_{IIC}}{3}}, \quad 0 \leq a_1 \leq L \quad (10)$$

Substituting the value of a_1 of equation (10) into equation (7), the displacement $u_1(P, \mathcal{G}_{IIC})$ is obtained:

$$u_1(P, \mathcal{G}_{IIC}) = \frac{PL^3}{48EI} + \frac{16}{P^2} \sqrt{EI} \left(\frac{B \mathcal{G}_{IIC}}{3} \right)^{3/2} \quad (11)$$

The elastic energy of the ENF specimen subjected to bending, **for** $L \leq a_2 \leq 2L$, is:

$$E_d = \int_0^L \frac{M_1^2}{2E(2l)} dx + \int_L^{a_2-L} \frac{M_2^2}{2E(2l)} dx + \int_{a_2-L}^{2L} \frac{M_2^2}{2E(8l)} dx = \frac{1}{2} P u_2 \quad (12)$$

$M_1(x)$ and $M_2(x)$ are the same of equation (6). Applying Castigliano's theorem in equation (12):

$$u_2 = (-3(3L - a_2)^3 + 8L^3) \frac{P}{96EI} \quad (13)$$

Thus, the stiffness K and the compliance C of the specimen with crack are obtained

$$K_2 = \frac{EI}{\frac{-3(3L-a_2)^3 + L^3}{32} + \frac{L^3}{12}} \quad C_2 = \frac{u_2}{P} = \frac{-3(3L-a_2)^3 + 8L^3}{96EI} \quad (14)$$

Using equation (14.b) in equation (2), \mathcal{G}_{IIC} can be estimated as:

$$\mathcal{G}_{IIC} = \frac{3P^2(3L-a_2)^2}{64BEI} \quad (15)$$

Rewriting (15) gives the crack length a_2 as a function of the critical energy relief rate:

$$a_2 = 3L - \frac{8}{P} \sqrt{\frac{BEI \mathcal{G}_{IIC}}{3}} \quad (16)$$

Or the crack length a_2 can be written according to equation:

$$a_2 = 3L - a_1 \quad (17)$$

Substituting equation (17) into equation (13) gives the displacement $u_2(P, \mathcal{G}_{IIC})$:

$$u_2(P, \mathcal{G}_{IIC}) = \frac{PL^3}{12EI} - \frac{16}{P^2} \sqrt{EI} \left(\frac{B \mathcal{G}_{IIC}}{3} \right)^{3/2} \quad (18)$$

Table 1 show the principal equations of the proposed analytical model.

Table 1: Equations used to model the ENF test.

Test	a	$C(a)$	$u(P, \mathcal{G}_{IIc})$
ENF	$0 \leq a_1 < L$	$\frac{L^3}{48EI} + \frac{a_1^3}{32EI}$	$u_1(P, \mathcal{G}_{IIc}) = \frac{PL^3}{48EI} + \frac{16}{P^2} \sqrt{EI} \left(\frac{B \mathcal{G}_{IIc}}{3} \right)^{3/2}$
ENF	$L \leq a_2 \leq 2L$	$\frac{-3(3L - a_2)^3 + 8L^3}{96EI}$	$u_2(P, \mathcal{G}_{IIc}) = \frac{PL^3}{12EI} - \frac{16}{P^2} \sqrt{EI} \left(\frac{B \mathcal{G}_{IIc}}{3} \right)^{3/2}$

Note that the specimen transversal displacement is a function of the applied load (P) and the fracture toughness of bonded joints, in mode II (\mathcal{G}_{IIc}). The crack length not appear explicitly.

2.2 The CBBM Model

In order to overcome the difficulties of the measuring of the crack length during the test and other problems inherent to the ENF test, MOURA *et al.* [7] proposed the Compliance Based Beam Method - CBBM. This method is based on an equivalent crack length a_e and enables the \mathcal{G}_{IIc} value to be obtained through the utilization of P vs δ curve only, with no measurement of crack size during the ENF test. MOURA *et al.* [7] considers the effect of the Fracture Process Zone (FPZ) on the crack performance that the other methods ignore. Fig. 3.a illustrates the Fracture Process Zone and Fig. 3.b shows schematically an example of resistance curve generated, as a graphical result, of the application of the CBBM model. The expressions of CBBM can be accessed in APPENDIX C.

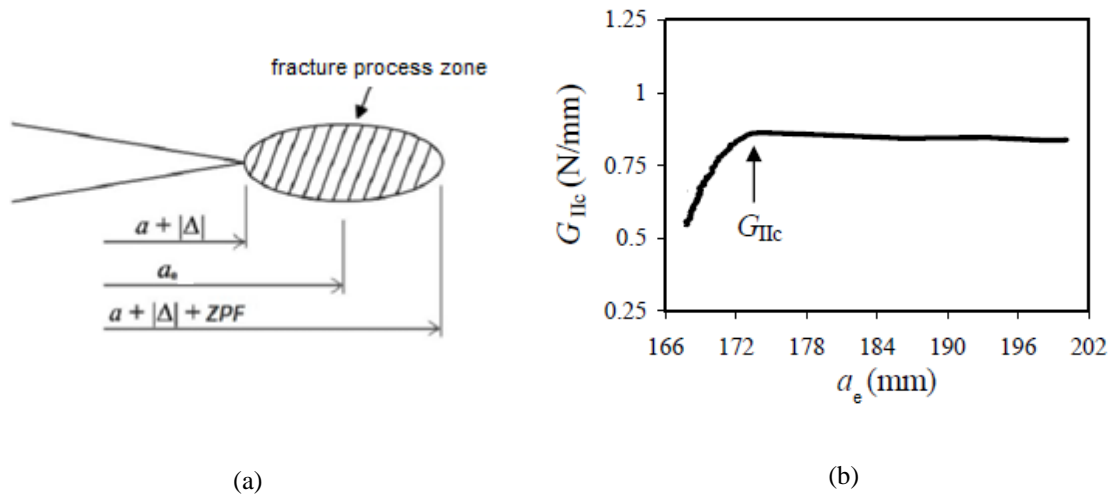


Figure 3: (a) Fracture Process Zone and (b) CBBM Resistance curve (R-curve). Adapted from MOURA *et al.* [7].

From equation (C.4), of APPENDIX C, it is possible to plot the resistance curve (R-curve) of \mathcal{G}_{IIc} vs a_e , shown schematically in Fig. 3.b, where the threshold of the curve determines the value of fracture toughness. As mentioned previously, there is no need to measure the crack during the test, only the data obtained from the P vs δ , the experimental test generates the R-curve, as a function of only the equivalent crack, a_e (not the physical one). According to MOURA *et al.* [7], the ascending part of the curve corresponds to the development of the ZPF in front of the crack tip. When it is fully developed; the crack begins to propagate, in order to obtain a level that defines the rate of critical energy. The propagation, or growth, of the crack during the test may occur in a stable or unstable manner and concluded that the growth of stable crack could be obtained to crack to $a \geq 0.7L$ (see Fig. 1.b to access the L meaning) and consequently the unstable growth would occur for $a < 0.7L$. In the next section the results will be presented.

3. RESULTS

In this section the two models, the proposed analytical and the CBBM models, are used with the input of ENF specimens experimental results.

The steel specimens substrate have the following geometry: overall length, $2L^* = 250$ mm (note that $2L^*$ is the specimen overall length and $2L$ the length between external supports of three-point bending appa-

ratus); each bar thickness, $h = 6,35$ mm; width, $B = 25$ mm and adhesive thickness, $t = 0,5$ mm. The used adhesive has the following characteristics: epoxy-based with a polyamine-based curing agent, NOVATEC NVT 201E, with tensile strength, $S_{ut} = 27$ MPa and shear rupture strength, $\tau_{rup} = 16$ MPa. Table 2 gives the values of the substrate yielding and adhesive rupture loads for the spacing between $2L = 200$ mm supports according to equations (B.3) and (B.9) of APPENDIX.

Table 2: Forces of substrate yielding and adhesive rupture.

force to onset yielding the substrate (P_1) (bending)	force to break (rupture) the adhesive (P_2) (shear)
7137 N	6773 N

Note that the force that yields the steel substrate P_1 must be bigger than the force that breaks the adhesive P_2 to produce valid results.

3.1 The analytical model application

Fig. 4.a shows the 25 kN material testing machine set up and Fig.4.b shows a specimen, used in experimental tests. It was setted two different crosshead speeds: a 3 mm/min and a 0.1 mm/min. The first one produced unstable crack propagation and the results were used together with the proposed analytical model. The second one, with a much slower crosshead speed, produced stable crack propagations and the results were used together with the existent CBBM model.



(a)

(b)

Figure 4: (a) Material Testing Machine set up and (b) specimen (lateral view).

To apply the analytical model, it is necessary to generate the crack propagation curves, for now on named the CP-curves, using equation (11) for $a < L$ and (18) for $a \geq L$. These curves represent the rate of evolution of fracture toughness as a function of the crack size during the test. Using a mathematical software, as MathCad, it was possible to generate the CP-curves, in function of \mathcal{G}_{IIC} values, as represented in Fig. 5.

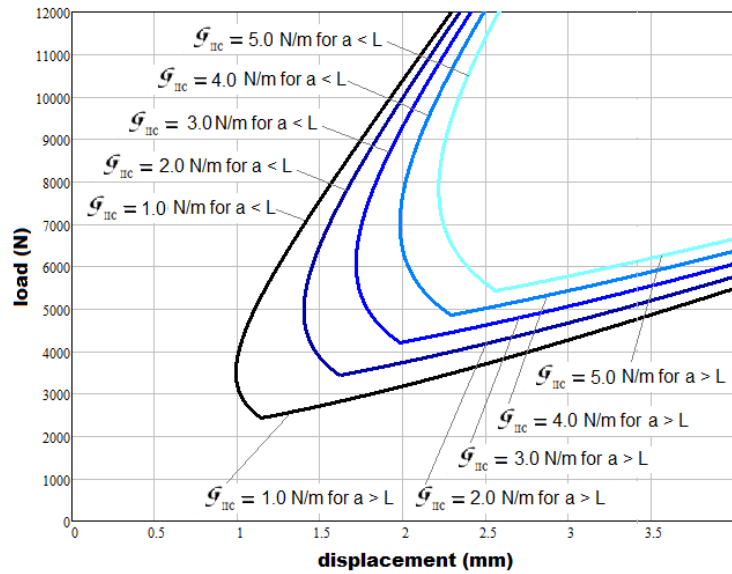
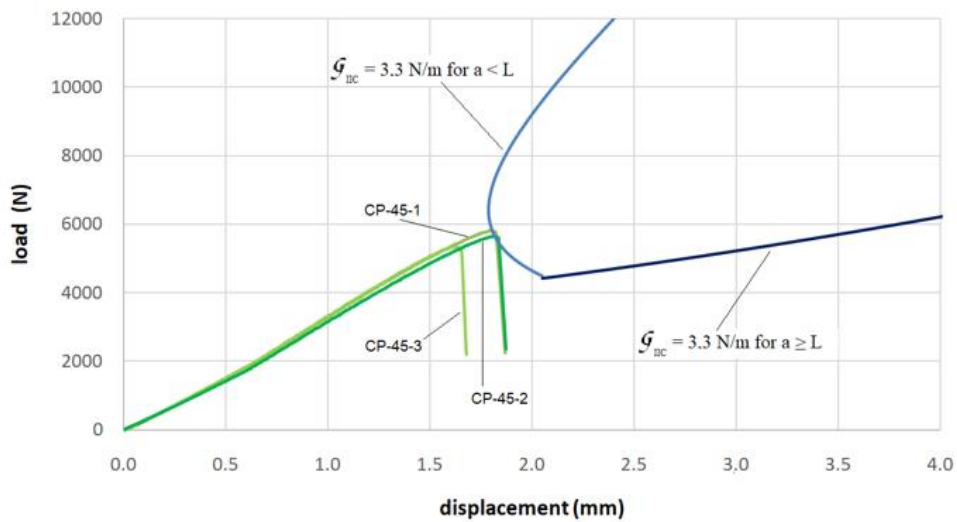


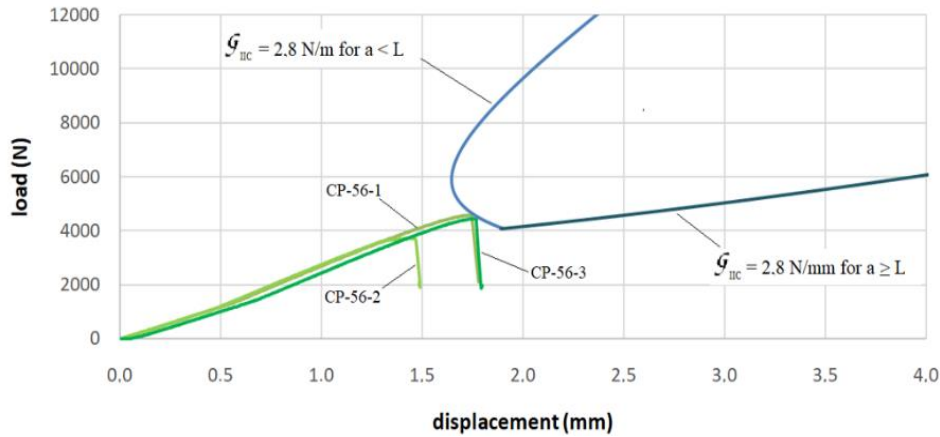
Figure 5: Example of CP-curves generated with the ENF specimens used in the research.

Note that as G_{IC} increases the CP-curves moves up and right, revealing that for the same initial crack length a_0 , high loads are necessary to reach adhesives with high G_{IC} . Fig. 6 shows two examples of application of the analytical model, for a crosshead speed of 3 mm/min, which crack propagation revealed unstable.

In Fig.6.a, the P vs u graphics of three ENF specimens were put together with a CP-curve. The single CP-curve that tangency the P_{max} point, in this case two of three specimens, is the searched curve, which correspond to the seek G_{IC} value. The same is valid for Fig. 6.b.



(a)



(b)

Figure 6: Results for analytical model: (a) for $a_0 = 45$ mm, $G_{IIc} = 3.3$ N/mm, and (b) for $a_0 = 56$ mm, $G_{IIc} = 2.8$ N/mm.

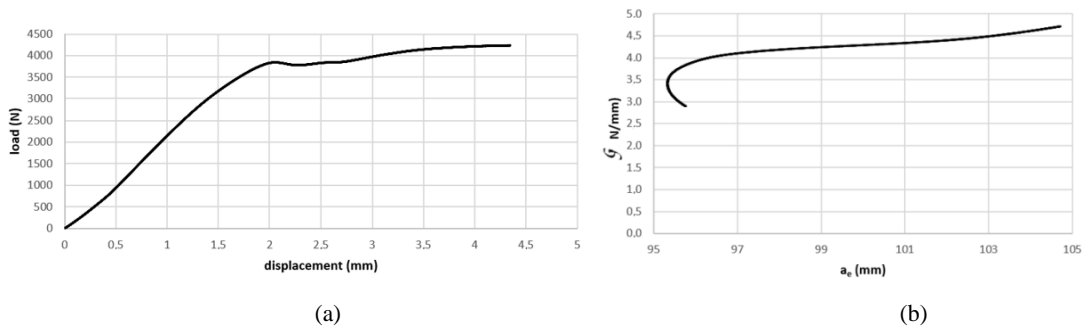
Note that for each a_0 (initial crack length), there were used three ENF specimens. For each test set it was considered the closest results, discarding the discrepant result. For Fig. 6.a (the specimens CP45-1 and CP45-2 were considered) and for Fig. 6.b (the specimens CP56-1 and CP56-3 were considered). For each specimen set, with $a_0 = 45$ mm and with for $a_0 = 56$ mm, the CP-curves, obtained using equations (11) and (18), were selected in order to touch the P vs u curves, obtained experimentally.

3.2 The CBBM model application

Two specimens, one with initial crack size $a_0 = 58$ mm (BC-5) and other with initial crack size $a_0 = 70$ mm (BC-9) were used for a crosshead speed of 0.1 mm/min. For these two specimens the cracks have stable propagation, that is, did not happen a sudden drop load the beginning of crack propagation. Bigger initial cracks (a_0) and low crosshead speed induced the stable crack propagation.

Figures 7 and 8 show the results of the application of the Compliance Based Beam Method - CBBM proposed by MOURA *et al.* [7], which is based on the equivalent crack length a_e , which considers the effect of the Fracture Process Zone (FPZ) ahead of crack tip. The possibility of estimating the G_{IIc} value through the P vs δ curve is a great advantage since the measurement of crack size during the test of ENF type specimens is quite difficult.

A mathematical software, as MathCad, could be used to treat the experimental data obtained in the experimental three point bending tests (see, Fig.7.a. and Fig. 8.a) to generate the G_{IIc} results (see, Fig.7.b. and Fig. 8.b).



(a)

(b)

Figure 7: Results for R-Curve model for $a_0 = 58$ mm: (a) load vs displac. and (b) $G_{IIc} \times a_e$, resulting in $G_{IIc} = 4.2$ N/mm.

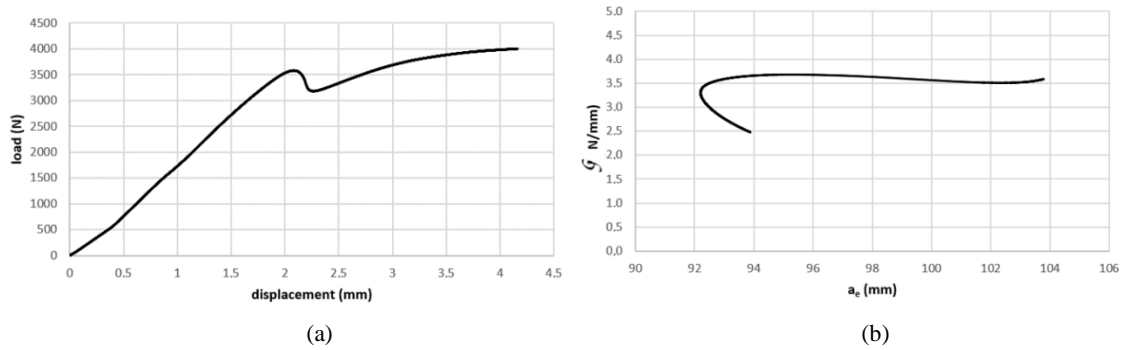


Figure 8: Results for R-Curve model for $a_0 = 70$ mm: (a) load vs displac. and (b) $G_{IIC} \times a_e$, resulting in $G_{IIC} = 3.7$ N/mm.

It can be observed from results, that to obtain stable crack propagation, to use the CBBM model for the estimation of G_{IIC} , it was necessary to conjugate large initial cracks with low crosshead speed.

4. CONCLUSIONS

The fracture toughness of the adhesive joint varies with the crack initial length, with larger initial cracks corresponding to smaller G_{IIC} values, for the same crosshead speed. Thus, the utilization of adhesive structural joint of a particular adhesive requires the assessment of its fracture toughness behavior for various initial cracks, for a particular transversal loading rate.

The proposed analytical approach, based in damage model, produced fracture toughness experimental results more conservative than the CBBM model ones, but it should be noted that for these two approaches it was used very different crosshead speeds, up to 30 times of difference, probably contributing for this discrepancy.

The specimens tested had quite different behavior as the initial crack sizes and crosshead speed were modified. The results obtained showed that specimens that are submitted to a lower crosshead speed, the greater the chances of stable propagation with ENF specimens three-point bending tests.

The utilization of two different approaches, without the necessity of crack length measurement, could access the fracture toughness of adhesive structural joints G_{IIC} for both, unstable and stable cracks.

5. REFERENCES

- [1] CASTRO, JAIME T.P., MEGGIOLARO, M.A. Fadiga - Técnicas e Práticas de Dimensionamento Estrutural sob Cargas Reais de Serviço – Volume II, Lexington, KY USA, 2009.
- [2] ALLIX, O., LADEVÉZE, P., CORIGLIANO, A. “Damage Analysis of Interlaminar Fracture Specimens”, Composites Structures, [https://doi.org/10.1016/0263-8223\(95\)00002-X](https://doi.org/10.1016/0263-8223(95)00002-X), v. 31, pp. 61-74, 2005.
- [3] DE BARROS, S., CHAMPANEY, L., “Crack Propagation Curves on Flexure Adhesion Tests”, Int. J. Journal of Structural Integrity, <https://doi.org/10.1108/IJSI-08-2011-0033>. v.4, n.3, pp. 396-406, 2013.
- [4] DE BARROS, S., CHAMPANEY, L., VALOROSO, N., “Numerical simulations of crack propagation tests in adhesive bonded joints”, Latin American Journal of Solids and Structures, <https://doi.org/10.1590/S1679-78252012000300002>. v.9, pp. 339-351, 2012.
- [5] DE BARROS, S., CHAMPANEY “Crack propagation tests: analytical and numerical approaches” In: H.S. da Costa Mattos & Marçílio Alves (Editors), Mechanics of Solids in Brazil 2009, pp. 183-192, 2009.
- [6] MOURA, M.F.S.F., CAMPILHO, R.D.S.G., GONÇALVES, J.P.M., “Pure mode II fracture characterization of composite bonded joints”, Int. J. of Solids and Structures, <https://doi.org/10.1016/j.ijsolstr.2008.12.001>. 46, pp. 1589-1595, 2009.

- [7] MOURA, M.F.S.F.; GONÇALVES, J.P.M., CHOUSAL, J.A.G., *et al.* “Cohesive and continuum mixed-mode damage models applied to the simulation of the mechanical behaviour of bonded joints”, *Int. J. of Adhesion & Adhesives*, v.28, pp. 419-426, 2008. <https://doi.org/10.1016/j.ijadhadh.2008.04.004>.
- [8] MOURA, M.F.S.F.; “Numerical simulation of the ENF test for the mode-II fracture characterization of bonded joints”, *J. of Adhesion Science and Technology*, v. 20, n.1 pp. 37-52, Apr.2006. <https://doi.org/10.1163/156856106775212422>.
- [9] MOURA, M.F.S.F., SILVA, M.A.L., MORAIS, J.J.L., *et al.* “A New Methodology for the Characterization of the Mode II Fracture of Pinus Pinaster Wood”, In: *Proceedings of the 5th International Conference on Mechanics and Materials in Design*, Portugal, July 2006.
- [10] BLACKMAN, B.R.K.; KINLOCH, A.J.; PARASCHI, M.; “The determination of the mode II adhesive fracture resistance, \mathcal{G}_{IC} , of structural adhesive joints: an effective crack length approach”, *Engineering Fracture Mechanics*, v. 72, issue 6, pp. 877-897, 2005. <https://doi.org/10.1016/j.engfracmech.2004.08.007>.
- [11] AZEVEDO, J. C. S.; Determinação da tenacidade à fratura em corte (\mathcal{G}_{IC}) de adesivos estruturais pelo ensaio End-Notched Flexure (ENF), Dissertação de M.Sc., Universidade do Porto, 2014.
- [12] ALVES, J. A., Determinação da Resistência à Fratura em Modo II de Juntas Coladas com Adesivo Estrutural, Dissertação de M.Sc., CEFET/RJ /PPEMM, Rio de Janeiro, RJ, Brasil, 2018.
- [13] GHIBIRGIU, D.; Determination of the toughness in mode II for different types of adhesive, Final Project in MIEM, Porto, Portugal, 2009.
- [14] ASTM D3433-99 Standard Test Method for Fracture Strength in Cleavage of Adhesives in Bonded Metal Joints. 1999.
- [15] CHAVES, F.J.P., SILVA, L.F.M., MOURA, M.F.S.F., *et al.* “Fracture Mechanics Tests in Adhesively Bonded Joints: A Literature Review”, *The Journal of Adhesion*, v. 90, pp.955-992, 2014. <https://doi.org/10.1080/00218464.2013.859075>.

ORCID

Jonnas Santos Alves	http://orcid.org/0000-0002-6155-0423
Paulo Pedro Kenedi	http://orcid.org/0000-0001-5563-843X
Silvio de Barros	https://orcid.org/0000-0002-2520-569X

6. APPENDIX

A. Strain Energy Method

Using the Strain energy method, in a 3-point bending arrangement (Fig. 2.a), it is possible to obtain the value of its displacement δ , the stiffness K and the compliance C . The potential energy E_d can be written:

$$E_d = \int_0^L \frac{M_1^2}{2EI_2} dx + \int_L^{2L} \frac{M_2^2}{2EI_2} dx \quad M_1 = \frac{P}{2}x \quad 0 \leq x < L, \quad M_2 = P\left(L - \frac{x}{2}\right) \quad L \leq x \leq 2L \quad (\text{A.1})$$

And can also be written as:

$$E_d = \frac{1}{2}P\delta \quad (\text{A.2})$$

From equations (A.1) and (A.2) the displacement u can be estimated:

$$\delta = \frac{PL^3}{6EI_2} = \frac{PL^3}{48EI} \quad \text{where} \quad I_2 = \frac{B(2h)^3}{12} = \frac{8Bh^3}{12} = 8I \quad (\text{A.3})$$

Where I_2 are the moment of inertia of the bar of $2h$ thicknesses. So, the stiffness of the beam subjected to bending can be obtained:

$$K = \frac{P}{\delta} = \frac{48EI}{L^3} \quad \text{and} \quad C = \frac{\delta}{P} = \frac{L^3}{48EI} \quad (\text{A.4})$$

B. Dimensioning of the specimen by Solid Mechanics

Analytical calculations are made for in order to have rupture in the adhesive before yielding on the steel specimen substrate, thereby determining the force required for the yielding of the substrate P_1 and the force required for the rupture of the adhesive P_2 .

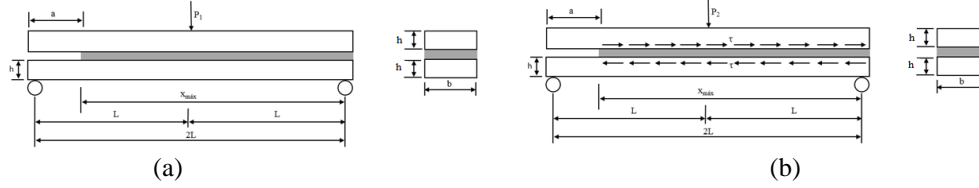


Figure B.1: Representation of an ENF test specimen, for preventing: (a) steel substrate yielding and (b) adhesive rupture.

From the Solid Mechanics, the maximum bending moment subjected to a bi-supported, as in Fig. B.1.a is:

$$M_{max} = \frac{P_1 L}{2} \quad (\text{B.1})$$

Thus, the maximum stress developed on the specimen substrate is:

$$\sigma_{m\acute{a}x} = \frac{M_{max} c}{I} = \frac{3 P_1 L}{4 b h^2} \quad (\text{B.2})$$

where, $c=h$ (h is considered to be half the thickness of the specimen) and $I = \frac{b \cdot (2h)^3}{12} \rightarrow I = \frac{2}{3} \cdot b h^3$. Thus, the transverse force P_1 which will produce the beginning of the steel bars yielding, for $\sigma_{m\acute{a}x} = S_{y_{a\grave{c}o}}$:

$$P_1 = \frac{4 b h^2}{3 L} S_{y_{a\grave{c}o}} \quad (\text{B.3})$$

The transverse force, now renamed to P_2 (see Fig. B.1b), is estimated in sequence:

$$q_1 = \frac{VQ}{I} \quad \text{where } V = \frac{P_2}{2} \quad \text{and} \quad Q = \bar{y}A = \frac{h}{2}(bh) = \frac{bh^2}{2} \quad (\text{B.4})$$

$$\text{Thus: } q_1 = \frac{3 P_2}{8 h} \quad (\text{B.5})$$

$$\text{The estimative of horizontal force in the bonded region: } F_H = q_1 x \quad \text{or} \quad F_H = \frac{3 P_2}{8 h} x \quad (\text{B.6})$$

Where x is the length of the cast joint. So, the shear stress in the bonded joint is then estimated:

$$\tau_2 = \frac{3 P_2}{8 h} \frac{x}{b(2L-a)} \quad (\text{B.7})$$

The maximum shear stress will occur at $x = x_{\text{max}} = (2L - a)$:

$$\tau_{m\acute{a}x} = \frac{3 P_2}{8 b h} \quad (\text{B.8})$$

Thus, the transverse force P_2 which will produce rupture in the adhesive, (when $\tau_{m\acute{a}x} = \tau_{rup_{adhesive}}$) is:

$$P_2 = \frac{8}{3} \cdot b h \cdot \tau_{rup_{adhesive}} \quad (\text{B.9})$$

Therefore, the value of the transverse force P_1 that will cause the yielding of specimen, equation (B.3) as well as the value of the force of rupture of the adhesive P_2 , equation (B.9). Since P_1 and P_2 are the same load P of specimen it is possible to equals equations (B.3) and (B.9). To obtain the dimension $2L$, as a function of height h , yield strength of the carbon steel ($S_y = 531$ MPa) and the shear stress of the adhesive rupture ($\tau_{rup_{adhesive}} = 16$ MPa). The inequality signal was inserted in equation (B.10) so that the dimension $2L$ does not cause yielding in the specimen can be estimated (for this case, $2L \leq 210$ mm).

$$2L \leq h \frac{S_y}{\tau_{rup_{adhesive}}} \quad (\text{B.10})$$

C. Compliance Based Beam Method – CBBM

MOURA *et al.* [7] used the beam theory approach and considered that the two bars of the specimen act as two independent beams supporting each one half of the applied load, as shown in Fig. C.1, and the moment of inertia of each section of each the bar being 1/8 of the moment of inertia of the specimen. .

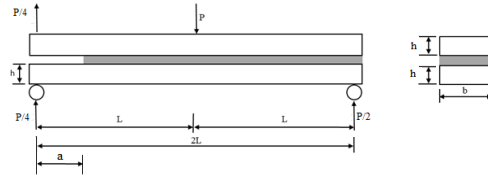


Figure C.1: Free body diagram of bonded joint subjected to transversal load. GHIBIRGIU [13]

The beam is analysed in 3 (three) parts ($0 \leq x \leq a$, $a \leq x \leq L$ and $L \leq x \leq 2L$), so the strain energy due to bending is written:

$$U_f = 2 \int_0^a \frac{(Px/4)^2}{2EI/8} dx + \int_a^L \frac{(Px/2)^2}{2EI} dx + \int_L^{2L} \frac{(Px/2 - P(x-L))^2}{2EI} dx \quad (C.1)$$

And the strain energy component due to shear is written:

$$U_c = 2 \int_0^a \int_{-h/2}^{h/2} \frac{\tau_{(c=h/2)}^2}{2G} B dy dx + \int_a^{2L} \int_{-h}^h \frac{\tau_{(c=h)}^2}{2G} B dy dx \quad (C.2)$$

where P is the transversal load; E and G are the longitudinal and transverse modulus of elasticity respectively and I is the moment of inertia of the specimen, respectively. B , a , h and L , are, respectively the width, the crack length, the semi-thickness and the length of specimen. Adding the two energy components U_f and U_c and applying Castigliano's theorem, the displacement at the point of application of the force P is obtained:

$$\delta = \frac{P(3a^3 + 2L^3)}{12EI} + \frac{3PL}{10GBh} \quad C = \frac{(3a^3 + 2L^3)}{12EI} + \frac{3L}{10GBh} \quad \mathcal{G}_{IIc} = \frac{9P^2 a^2}{16B^2 E h^3} \quad (C.3)$$

After a development (see MOURA *et al.* [7] for the details) the final equation is reached:

$$\mathcal{G}_{IIc} = \frac{9P^2}{16B^2 E_f h^3} \left[\frac{C_{corr}}{C_{ocorr}} a_0^3 + \frac{2}{3} \left(\frac{C_{corr}}{C_{ocorr}} - 1 \right) L^3 \right]^{1/3} \quad (C.4)$$

$$\text{where, } C_{corr} = C^* - \frac{3L}{10GBh} \quad C^* = \frac{(3a_e^3 + 2L^3)}{12E_f l} + \frac{3L}{10GBh} \quad a_e = a + \Delta_{a_{FPZ}} \quad E_f = \frac{3a_e^3 + 2L^3}{12l} \left(C - \frac{3L}{10GBh} \right)^{-1}$$